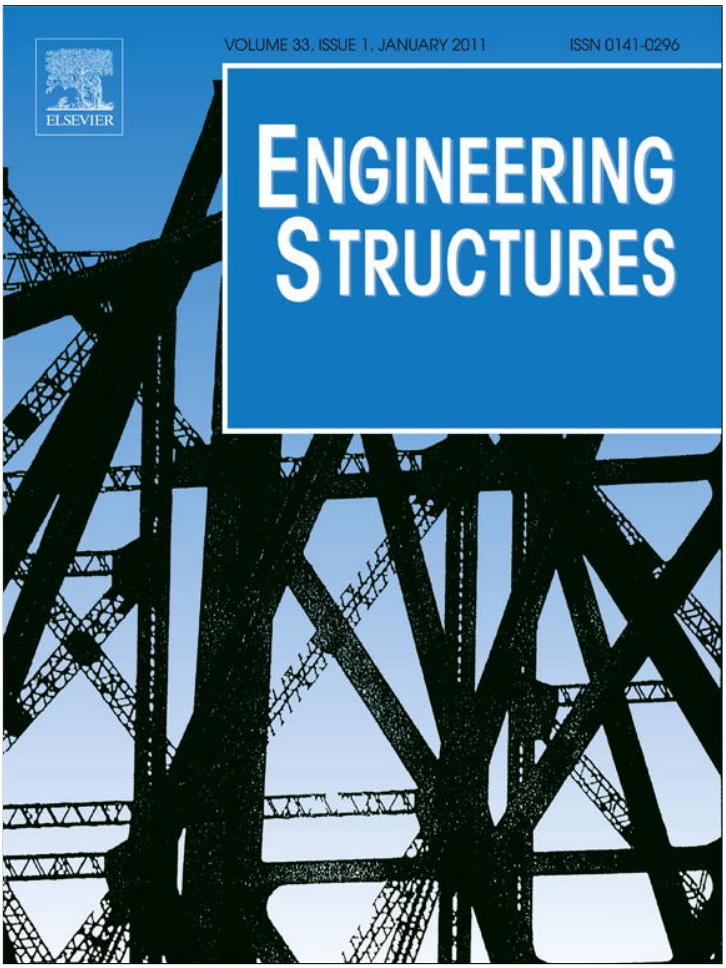

(This is a sample cover image for this issue. The actual cover is not yet available at this time.)

Engineering Structures 34 (2012) 21–32

Contents lists available at SciVerse ScienceDirect

Engineering Structures

journal homepage: www.elsevier.com/locate/engstruct

Horizontally curved steel bridge seismic vulnerability assessment

Junwon Seo [a,*], Daniel G. Linzell [b]

[a] Bridge Engineering Center, Department of Civil, Construction, & Environmental Engineering, Iowa State University, Ames, IA 50011, United States
[b] Protective Technology Center, Department of Civil and Environmental Engineering, The Pennsylvania State University, University Park, PA 16802, United States

ARTICLE INFO

Article history:
Received 25 April 2010
Revised 1 September 2011
Accepted 2 September 2011

Keywords:
Earthquake
Vulnerability
Curved
Bridges
Monte Carlo simulation
Response Surface Metamodels

ABSTRACT

Most computational research related to steel bridge seismic vulnerability has focused on statistical extrapolation of analysis results for individual straight bridges. However, there has been a steady growth in the use of horizontally curved steel bridges in highways and interchanges in large urban regions. Given the large number of curved steel bridge structures in use in the US and abroad, with some of those structures being located in seismic zones, the feasibility of examining the effects of curvature on bridge vulnerability should be investigated. In this study, the seismic performance characteristics of an existing inventory of horizontally curved, steel, I-girder bridges located in Pennsylvania, New York, and Maryland were used to generate fragility curves. Representative fragility curves for horizontally curved, steel, I-girder bridges were estimated using Response Surface Metamodels (RSMs) in conjunction with Monte Carlo simulation. The methodology was used to construct fragility curves for select bridge components (bearings, columns and abutments). The curves were generated for four different, preexisting, performance states that represented slight, moderate, extensive, and complete damage under varying levels of earthquake intensity. The generated fragility curves provided information related to seismic response of the bridge inventory that was investigated, such as radial deformations at the bearings being the most susceptible component to seismic loads.

1. Introduction

Past research has demonstrated that the loss of one or multiple bridges in a transportation network can hamper recovery activities and can severely impact the economy of the region encompassing that network [1]. Bridges are known to be one of the most vital, and vulnerable, components of any transportation network. Therefore, in many instances during an extreme event, such as an earthquake, it is vital that bridges affected by the event remain operational. The generation of vulnerability functions in the form of fragility curves is a common approach for assessing bridge seismic vulnerability [1–6]. A fragility curve provides a conditional probability that gives the likelihood that a structure, or one of its components, will meet or exceed a certain level of damage for a given ground motion intensity. Information provided from a fragility curve can be used for prioritizing bridge retrofits, for pre-earthquake planning and for post-earthquake response and evaluation. These curves usually account for a multitude of sources of uncertainty related to estimating seismic hazards, including bridge characteristics and bridge type and configuration.

Fragility curves have been generated using various approaches. Expert based fragility curves are typically generated using earthquake damage and loss estimates for industrial, commercial, residential, utility and transportation facilities and are based on expert opinions [7]. As a result, this methodology naturally involves subjectivity, resulting in a high level of uncertainty. Empirical fragility curves are generated from actual earthquake data and give a general idea about the relationship between structure damage levels and ground motion indices [2,8]. Basoz and Kiremidjian [8] initially developed empirical fragility curves for bridges using Peak Ground Accelerations (PGAs) derived from damage data from the 1989 Loma Prieta and 1994 Northridge earthquakes. They used logistic regression analysis to generate the fragility curves based on a damage probability matrix for multiple span bridges. Analytical fragility curves are produced based on numerical simulations that consider different levels and types of ground motions [3–6] and are generally developed using seismic response from nonlinear time history analyses [3–6]. Shinozuka et al. [9] showed that analytical fragility curves are in reasonably good agreement with empirical curves. Due to the combination of the aforementioned subjectivity associated with defining earthquake damage states from expert opinions and the paucity of actual bridge damage data associated with seismic events, expert based and empirical fragility curves have rather limited application. Conversely, the creation of analytical fragility curves continues to increase in both academic and practical settings due to the improvement in analytical and statistical modeling tool accuracy and speed.

* Corresponding author. Tel.: +1 515 294 9501; fax: +1 515 294 0467.
E-mail addresses: jseo@iastate.edu (J. Seo), dlinzell@engr.psu.edu (D.G. Linzell).

0141-0296/$ - see front matter © 2011 Elsevier Ltd. All rights reserved.
doi:10.1016/j.engstruct.2011.09.008

Although the generation of analytical fragility curves using nonlinear time history finite element analyses has been recognized as a relatively reliable technique, these types of models tend not to be included in probabilistic analysis frameworks. This is because an excessive amount of computational cost has historically been associated with generation and implementation of nonlinear analyses for a large population of complex bridges under a varying range of seismic hazards. Recently, analytical seismic fragility curves have been generated for a population of structures at low computational cost using Response Surface Metamodels (RSMs) approximations. RSMs, which can be described as mathematical polynomial regression functions [10], give the probability of failure of bridges as a function of the random variables that affect the seismic response [11]. RSMs have been efficiently used in connection with probabilistic approaches (e.g., the First Order Reliability Method, Monte Carlo simulation) to generate seismic fragility curves for concrete, steel, and masonry buildings and concrete bridges [11–15].

While most research that produced analytical fragility curves with RSMs has focused on building groups [12–15], some work has been completed that has focused on straight, concrete bridges [11]. It has been reported that horizontally curved steel bridges make up a measureable portion of the approximately 597,500 bridges in United States road network [16] and that over one third of all constructed steel bridges are curved [17], numbers which continue to increase. Given the increasing number of curved steel bridge structures in use, with some of those structures being located in seismic zones, examination of the effects of curvature on bridge seismic performance, with a focus on bridge fragility, should occur. A number of analytical and experimental studies have been conducted related to the complicated static and dynamic behavior of horizontally curved steel girder bridges [18–21], but studies that attempt to generate seismic fragility curves for these bridges have not been performed.

To adequately and efficiently assess the seismic vulnerability of an inventory of curved steel bridges, seismic fragility curves were generated using statistical examination of seismic response from RSMs developed from models that predicted the behavior of a group of actual curved steel bridges. Fragility curves were created using the RSMs in connection with Monte Carlo simulations with original bridge statistics supplied from an inventory of horizontally curved, steel, I-girder bridges in Pennsylvania, New York, and Maryland. This paper focuses on detailed description of the fragility curve generation and application process, with a focus on computational work involved to create the curves.

2. Seismic vulnerability methodology using RSMs

2.1. RSM description

RSMs can be described as statistically derived polynomial functions that determine approximate parameters for an unknown function, $y(x)$, used to describe response variables of interest. The values of this function in the neighborhood of a defined point, say x_0, are found based on values of y obtained using appropriate numerical experiments, such as Central Composite Design (CCD). It is common to use RSMs that limit the order of their polynomials to two [10] since low-order RSMs require fewer experiments to be performed [11,22] and have been shown to accurately predict dynamic response [22]. RSM functions used in this study can be expressed as follows [10]:

$$y = \beta_0 + \sum_{i=1}^{k} \beta_i x_i + \sum_{i=1}^{k} \beta_{ii} x_i^2 + \sum_{i=1}^{k-1} \sum_{j>i}^{k} \beta_{ij} x_i x_j + \varepsilon \quad (1)$$

where y is the dependent variable, such as seismic response; x_i, x_j are independent input parameters, such as curved bridge radius of curvature; β_0, β_i, β_{ii}, β_{ij} are coefficients to be estimated from sets of seismic responses and independent input variables; k is the number of input variables; and ε is the term representing the bias of fit.

The minimum number of experiments necessary for determining β is equal to the number of the parameters. This number must be increased if the estimate of β is to be sufficiently reliable; accordingly, a compromise must be established between the two competing requirements of accuracy and economy. The choice of a rational design for the experiments is thus an essential part in the RSM development procedure. Use of CCD during RSM generation has satisfied the requirements of accuracy and economy [10]. CCD involves establishing three levels for each of the input variables k and then carrying out $2^k + 2k + 1$ experiments corresponding to viable variable combinations. CCD can explore the effects of the variations of both single variables and the interaction of multiple variables and accordingly permits an accurate estimate of actual behavior using a quadratic RSM function [10].

2.2. Methodology overview

The developed RSMs were utilized to both compute seismic response and generate seismic fragility curves for a target bridge inventory. To reduce the number of time-consuming nonlinear time history analyses, an optimal number of finite element models used for seismic analysis of complex bridge structures (i.e., curved bridges) were determined using CCD. To compute seismic response in an efficient manner, the RSMs were then developed using least-squares regression analysis based on optimal bridge model results from nonlinear time history analyses. Uncertainties related to bridge parameters that heavily influenced the seismic response were treated via the RSMs, instead of via the nonlinear time history analyses. The created RSM functions were initially used to compute seismic response of select bridge components. Seismic fragility curves were then created by reutilizing the RSMs in conjunction with Monte Carlo simulations to examine a random set of seismic inputs and curved bridge geometries. Monte Carlo simulations, which obtain an approximate probability distribution for the desired outcomes (i.e., seismic response) for the target bridge inventory, were selected because they have been successfully applied to bridge fragility curve generation in conjunction with RSMs in the past.

A schematic of the process used to generate the fragility curves, which included the aforementioned RSMs, is shown in Fig. 1. The first step shown in Fig. 1 was the completion of an inventory analysis of a select group of horizontally curved bridges. This analysis assisted with defining important parameters for future RSMs and involved defining appropriate values for both RSM inputs and outputs. Input parameters, which consisted of macro- (e.g. geometric and structural) and micro- (e.g. material) level parameters, were determined based on characteristics of the selected bridge inventory and on information from past steel bridge research [18,20,21]. Macro-level parameters, which are typically representative of global geometric parameters [16], contained variables identified from past parametric studies [18,20,21] as having dominant influence on curved bridge seismic response. Micro-level parameters were shown to have some effect on bridge seismic response but were less influential than the macro-level parameters [11]. Sample curved bridge macro-level parameters included radius of curvature and cross-frame and girder spacing [18,20,21]. The Young's modulus for steel and the concrete compressive strength were considered micro-level parameters [13]. Ranges for each macro- and micro-level parameter were based on statistical data from the bridge inventory examined for this study, which allowed for development of probability distributions for the parameters.

Step 2 began with identification of optimal parameters that assisted with defining the RSMs. Optimal parameters were defined

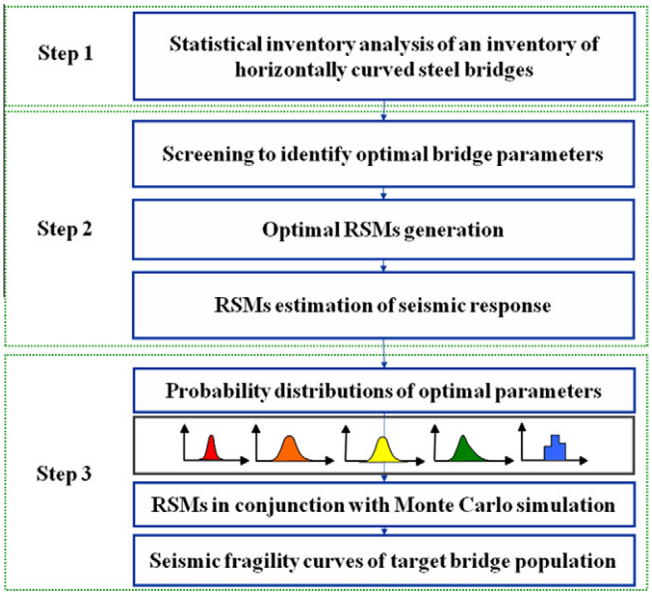

Fig. 1. Fragility curve generation using RSMs.

as those macro- and micro-level parameters that heavily influenced seismic response from nonlinear time-history analyses of twenty 3-D curved bridge models under a representative ensemble of synthetic ground motions [23] in OpenSees [24]. Plackett–Burman Design (PBD) was used to assist with identifying the optimal parameters [10].

The second item in Step 2 focused on generation of the first set of RSMs, those that were used to predict seismic performance, using statistical examination of output from the OpenSees models. Optimal seismic performance output parameters, such as peak radial bearing deformations, were established by applying CCD to combinations of RSM inputs and utilizing first order regression of the combinations. Output parameters of interest have been used for fragility curve development in previous studies [3–6,25–27] and included: (1) peak translations at the bearings, which included radial and tangential components; (2) peak abutment deformations directly adjacent to the bearing seats, which also included radial and tangential components; and (3) column curvature ductility, which refers to the ratio of the curvature in the column that causes first yield of the outer most reinforcing steel to the maximum curvature demand of the column during a seismic event [5]. For the column curvature ductility calculation, moment–curvature plots for the bridge columns were generated via OpenSees to capture their maximum curvature for a range of seismic loadings. Column curvature ductility was then calculated based on the maximum curvature and evaluated via comparisons to specified column ductility damage states from FEMA and other past work [3–6].

The last task associated with Step 2 involved producing seismic performance values for the selected output parameters using the generated RSMs. Peak Ground Acceleration (PGA) was used as the main input indicator of seismic performance. These performance values would then be used in the generation of seismic fragility curves in the final step.

The final step, Step 3 in Fig. 1, focused on development of the fragility curves for the bridge inventory that was examined. It initiated with determination of appropriate probability distributions for optimal input parameters for the region that was studied. Probability distributions were selected based on aforementioned statistical analyses of the bridge inventory. These distributions were applied to the generated seismic performance RSMs and Monte Carlo simulation was employed to establish a set of fragility curves. Resulting output parameters were compared against previously developed FEMA performance states [25] for structures under earthquake loadings and exceedance probabilities were numerically computed, again using Monte Carlo simulation. Qualitatively, the FEMA performance states represented slight, moderate, extensive, and complete earthquake damage levels. Corresponding quantitative states for the output parameters of interest were 2obtained from past research [3–5]. A single exceedance probability value represented one point at a specific earthquake intensity level on a fragility curve. The process was repeated over a specified range of earthquake intensities, with the range being supplied using Monte Carlo simulation, and fragility curves that plotted the variation in exceedance probability for a range of earthquake intensity levels were obtained for each FEMA performance state.

3. Application

More detail on application of the outlined methodology is provided in the sections that follow. This information includes details on models used to generate the RSMs along with presentation of the RSMs that were generated.

3.1. Horizontally curved bridge inventory

An inventory statistical analysis was completed using available construction plans collected from the Maryland Department of Transportation (MDOT), the New York Department of Transportation (NYDOT) and the Pennsylvania Department of Transportation (PennDOT) to establish a statistical basis for RSM generation. This region was selected because bridges in proximity to the researchers were largely designed without seismic detailing due to a low to moderate level of seismicity. Three hundred and fifty-five horizontally curved steel I-girder bridges, both with and without skew, were included in the inventory. Of these 355 bridges, 129 were without skew (36%) and 226 were a combination of skewed and curved steel I-girder bridges (64%). This study focused on curved bridges without skew.

Curved steel I-girder bridges that remained in the inventory were divided based upon the number of horizontal curves included in their design geometry. These included bridges containing single, two or more than two horizontal curves. Fig. 2 details the distribution of bridges with respect to number of horizontal curves and indicates that, of the 129 curved I-girder bridges, 99 of them were constructed using a single horizontal curve. All RSM generation and evaluation work was based on data from these 99 bridges. An elevation and typical section from a representative horizontally curved steel I-girder bridge is shown in Fig. 3. The bridge has two spans and a single multi-column bent. The bridge slab is supported by steel girders resting on steel rocker and spherical bearings.

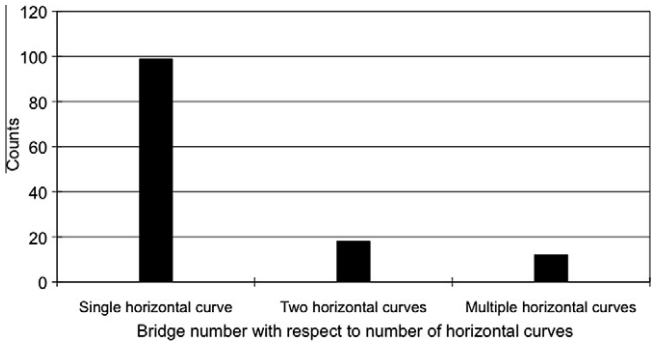

Fig. 2. Bridge statistics, number of horizontal curves.

Important macro-level parameters were identified by looking at National Bridge Inventory (NBI) data [16] and investigating additional characteristics from the bridge inventory plan sets. Key macro and micro-level parameters were identified using existing literature [11,12,16,18,21] coupled with understanding of curved bridge behavior. NBI data provided the following geometric, macro-level parameter information: (a) number of spans; (b) maximum span length; (c) deck width; and (d) vertical underclearance (equated to pier height). Additional macro-level parameters specific to curved bridges included radius of curvature and girder and cross-frame spacing and subsequent ranges were obtained from the bridge plans [18,20,21,28]. Micro-level parameter ranges, which included concrete and steel material properties, were also obtained from the bridge plans.

To account for inherent uncertainty associated with the selected macro- and micro-level parameters, these parameters were considered random variables for all probabilistic work associated with RSM development. Table 1 summarizes the final macro- and micro-level parameters that were included in the study.

3.2. 3-D computational models

As was stated previously, 3-D computational models were created in OpenSees [24]. Previous research indicated that, for the models that were created, the superstructure could be modeled elastically under seismic loads while the substructure should be modeled as both geometrically and materially nonlinear [3–6]. Nonlinear time history analyses of the models were used to produce important output data (e.g., tangential and radial bearing deformations) for RSM generation.

Models were created using previously published approaches [4–6]. The superstructure was modeled using frame elements to represent girder flanges and webs and the concrete deck with rigid link elements being used to mimic composite action and couple the top and bottom flange elements. Cross-frames were idealized using truss elements connected to the girder flange elements. Nominal material properties were used for both the concrete and steel when initially developing the models. However, it should be noted that variation in the properties was considered in models used for RSM generation. Bearings that developed restraint against tangential, and radial deformations were used for all girders in the curved bridge models. Since bearing seismic response was expected to be nonlinear, their moment-rotational behavior was explicitly modeled.

The substructure was also modeled based on information from previous research [5] and included the pier caps, columns, foundations, and abutment seats and backwalls. OpenSees displacement beam-column elements, which included reinforcement effects and could represent geometrical and material nonlinearities, were used to model the pier caps and pier columns. Each fiber within pier caps and pier columns was modeled with a proper stress–strain relationship depending on the confined, the unconfined concrete regions, and the longitudinal steel reinforcement. The relationships were incorporated in the nonlinear time-history analysis to result in appropriate moment–curvature responses by using OpenSees. OpenSees zerolength elements with nonlinear translational and rotational springs were used to represent the ef-

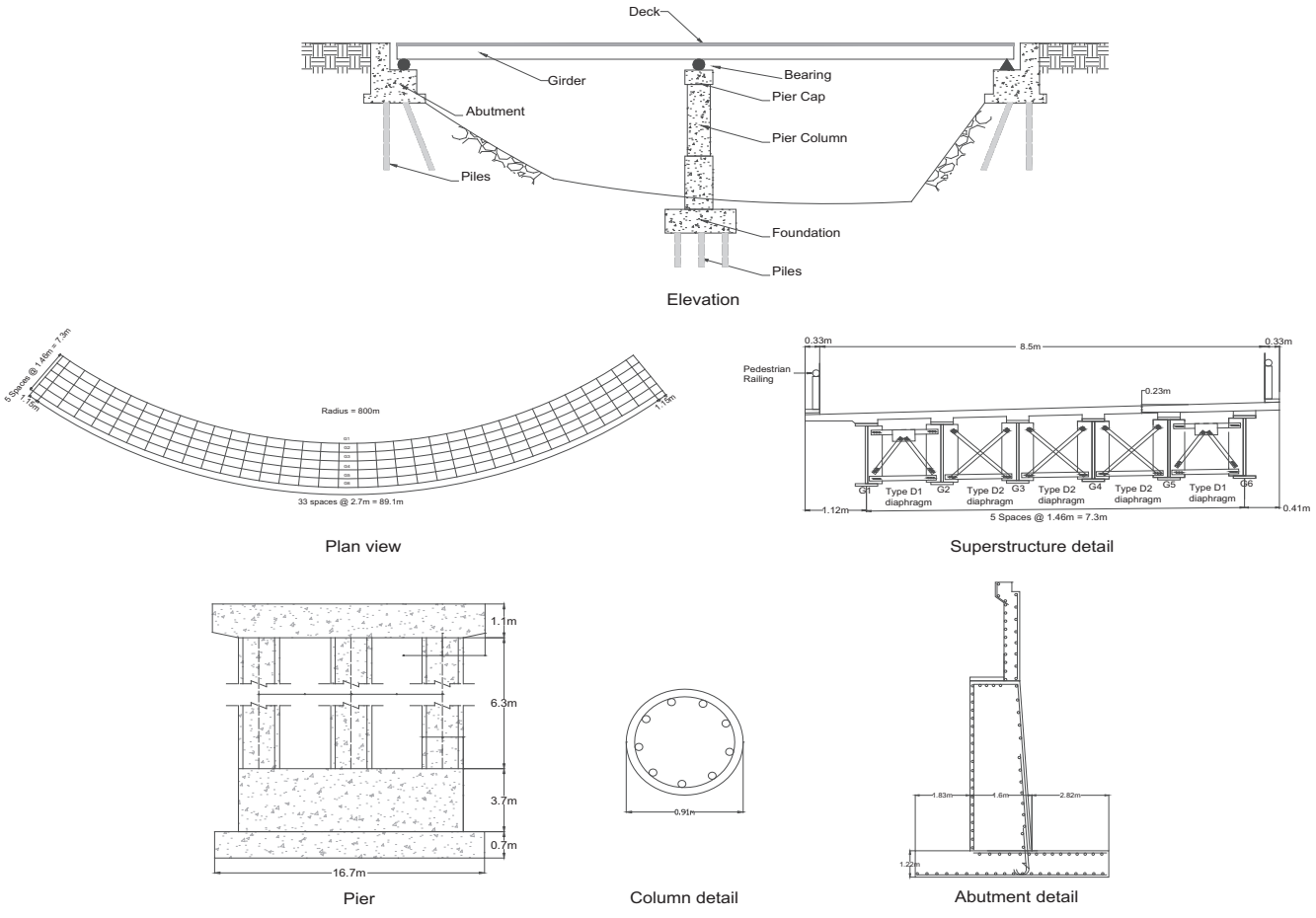

Fig. 3. Representative horizontally curved, steel, I-girder bridge.

Table 1
Horizontally curved steel I-girder bridge parameters.

Parameter Category		Parameters	Lower Level	Upper Level
			−1	1
Macro parameters	*X*1	Number of span	1	3
	*X*2	Maximum span length, m	15.2	91.4
	*X*3	Deck width, m	8.5	17.3
	*X*4	Maximum column height, m	10	32.3
	*X*5	Radius of curvature, m	240	3492
	*X*6	Girder spacing, m	1.46	3.23
	*X*7	Cross-frame spacing, m	2.7	7.31
Micro parameters	*X*8	Damping ratio	0.2	0.8
	*X*9	Concrete compressive strength, MPa	20.7	34.1
	*X*10	Concrete tensile strength, MPa	1.7	2.7
	*X*11	Concrete Young's modulus, MPa	17	31
	*X*12	Steel reinforced bar Young's modulus, MPa	192,920	206,700
	*X*13	Steel reinforced bar Yield strength, MPa	289.4	345

fect of soil-structure interaction when modeling the foundations and abutments.

3.3. Optimal RSM parameter identification

Creation of the initial set of RSMs utilized information from Table 1 in conjunction with a screening process that helped establish which of those parameters and their combinations was statistically significant and necessary in the final RSM polynomials. Fig. 4 details the RSM parameter screening process. Identification of optimal RSM parameters was accomplished using a combination of PBD and statistical tools that employed least-squares regression of the input variable combinations listed in Table 1. A two-level design used minima and maxima of the 13 input variables to form the PBD space table [10]. As a result of the use of the PBD space table, the 20 PBD-based bridge models were generated from the 13 input variables. These 20 combinations replaced representative bridges that could be selected from the 99 bridge inventory. Table 2 details the sample 20 combinations. Synthetic ground motions, which were developed based on statistical analysis of ground motions from past research [23], were used as the loadings for the computational models. Nonlinear time-history analysis of the twenty combinations was then completed.

The RSM parameter identification method systematically incremented each macro- and micro-level input variable and computed resulting important seismic response quantities, with combined macro and micro-level input variable effects examined using PBD. Resulting output was rank-ordered and yielded a Pareto optimal solution [29] that highlighted the individual and cumulative influence of PBD variables on the seismic response output items of interest, which again included: (1) peak translations at the bearings, which included radial and tangential components; (2) peak abutment deformations directly adjacent to the bearing seats, which included radial and tangential components; and (3) column curvature ductility. Fig. 5 contains representative Pareto optimal plots for peak bearing radial deformations. The bars represent individual contributions to the seismic response and demonstrate how each input parameter contributed to radial deformation. The solid line, in turn, represents a cumulative contribution to the overall response and demonstrates which input parameters most signifi-

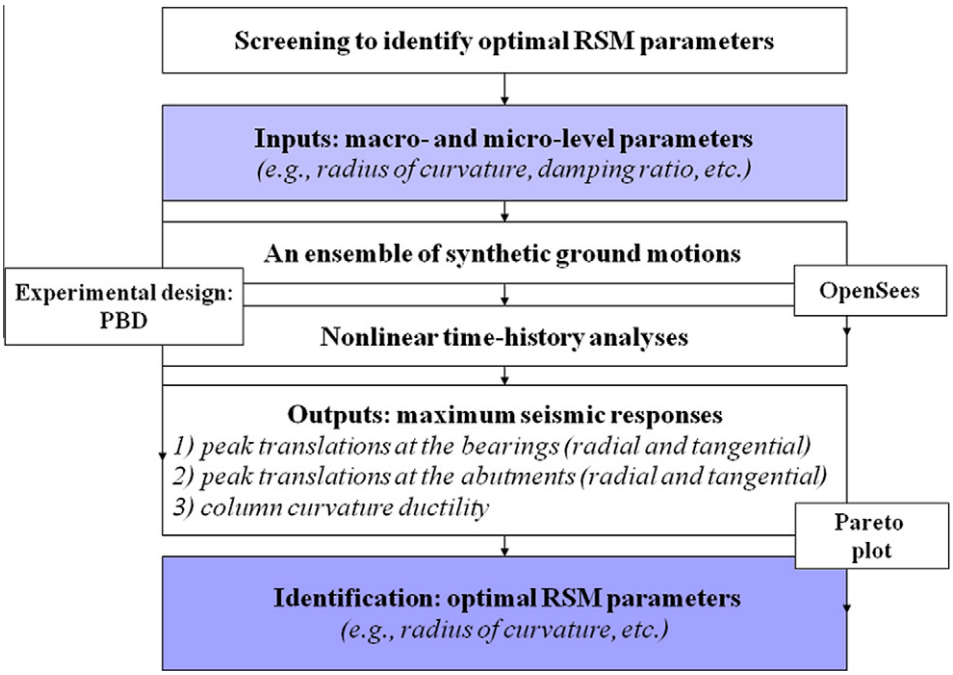

Fig. 4. Optimal RSM parameter screening process.

Table 2
Example Plackett–Burman combinations.

Curved bridge combinations	X1	X2	X3	X4	X5	X6	X7	X8	X9	X10	X11	X12	X13
1	−1	−1	−1	−1	1	−1	−1	1	−1	−1	1	1	1
2	−1	1	1	−1	1	−1	−1	1	1	1	1	−1	1
3	−1	1	−1	1	−1	−1	−1	1	1	−1	−1	1	−1
...	...	...	...	...	...	...	...	...	...	...	...	...	...
18	1	1	1	1	1	−1	1	−1	−1	−1	−1	1	1
19	−1	−1	1	1	1	−1	1	−1	1	−1	−1	−1	−1
20	−1	−1	1	1	−1	1	−1	−1	1	1	1	1	−1

Note: lower level (−1) and upper level (1).

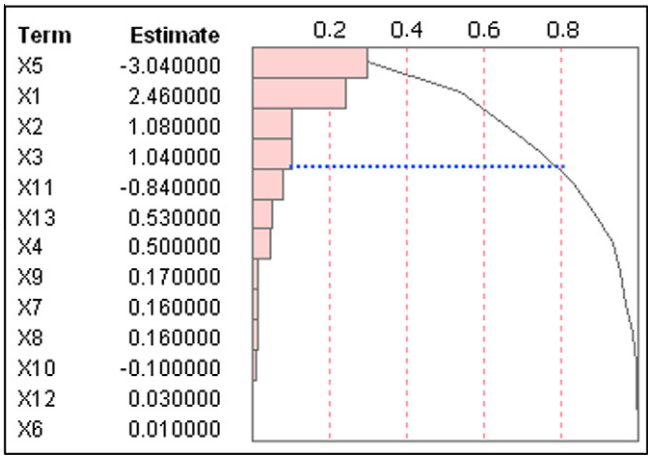

Fig. 5. Sample Pareto optimal plot.

cantly contribute to the response. In general, when identifying significant seismic parameters using this approach, those that contributed more than 80% of the seismic response are deemed significant [29,30]. For example, the results from Fig. 5 indicate that variables $X1$, $X2$, $X3$ and $X5$ were the parameters that had more than 80% influence on bearing radial deformations. Results from the selected output variables showed that, though the relative significance of the various parameters may change for a given output variable, optimal parameters to use in the RSM polynomials to predict seismic response were determined to be the number of spans ($X1$), maximum span length ($X2$), radius of curvature ($X5$), girder spacing ($X6$), and cross-frame spacing ($X7$). Pareto optimal plots of the other output variables can be found elsewhere [31].

3.4. RSM seismic response estimation

The RSMs were formulated using the five identified influential bridge parameters from the screening analysis and they considered each parameter effect independently and their interaction using three level CCD [10]. Table 3 displays these five input parameters and their corresponding upper, center and lower level values needed for three level CCD. RSMs for seismic response were developed with these five parameters via CCD, with PGA being selected as the output parameter from the RSMs due to its common use as an earthquake intensity indicator measure for fragility development [5]. As a result, a total of 45 curved bridge combinations were examined based on the five optimal parameter combinations coupled with varying earthquake intensity levels as outlined in Table 4. To demonstrate how a response calculation was accomplished for the CCD combinations, one sample combination is discussed. The first combination contained $X1 = -1$, $X2 = 1$, $X5 = -1$, $X6 = -1$, $X7 = -1$, and $X_{eq} = -1$. The set was interpreted as a simple span horizontally curved steel I-girder bridge that has a maximum span length of 91.4 m, a radius of curvature of 240 m, a girder spacing of 1.46 m, and a cross-frame spacing of 2.7 m. This bridge was then subjected to an ensemble of synthetic ground motions discussed below having an average PGA of 0.1 g.

Table 4
Example CCD combinations.

Curved bridge combinations	X1	X2	X5	X6	X7	X_{eq}
1	−1	1	−1	−1	−1	−1
2	−1	1	1	−1	1	−1
3	−1	1	1	−1	−1	1
...	...	...	...	...	...	...
43	0	0	0	0	0	0
44	0	−1	0	0	0	0
45	0	0	0	−1	0	0

Note: lower level (−1), center level (0), and upper level (1).

To examine seismic response for a broader range of earthquake scenarios, an ensemble of synthetic ground motions [23] randomly extracted based on the Latin Hypercube sampling (LHS) technique for three-level PGAs were used. These ground motions had different PGA values and frequency contents and resulted in different outputs from the nonlinear time history analyses for items of importance, such as peak radial deformations. In this study, RSMs were generated for a mean value and a standard deviation of ground motions to treat their uncertainty. The RSMs mean was generated using input parameters and mean output values, whereas the RSMs standard deviation was developed using input parameters and output standard deviations. Because the selected ground motion suite contained unidirectional motions, the unidirectional ground motions were applied to curved bridge models in the longitudinal direction and then in a transverse direction with respect to the bridge model in OpenSees. Fig. 6 shows representative directions along with the synthetic ground motion and spectral accelerations that were used [23].

Table 3
Optimal parameters for seismic fragility RSM generation.

Optimal parameters for RSMs	Lower level (−1)	Center level (0)	Upper level (1)
$X1$: number of spans	1	2	3
$X2$: maximum span length, m	15.2	53.3	91.4
$X5$: radius of curvature, m	240	1866	3492
$X6$: girder spacing, m	1.46	2.35	3.23
$X7$: cross-frame spacing, m	2.7	5.01	7.31
X_{eq}: Peak Ground Acceleration, g	0.1	0.55	1

Least-square regression was used to develop the final polynomial means and standard deviations for the RSM functions. Sample RSM polynomials that address variations of the mean and standard deviation for peak radial deformation at a bearing are shown in Eqs. (2) and (3):

$$\begin{aligned}\hat{y}_{\mu|\text{radial-bearing}} &= 32.340 + 1.638x_1 - 0.355x_2 - 3.889x_5 \\ &+ 0.040x_6 + 0.748x_7 + 42.851x_{eq} - 0.178x_1^2 \\ &+ 0.648x_1x_2 + 0.424x_2^2 + 0.379x_1x_5 \\ &+ 0.113x_2x_5 + 2.480x_5^2 + 0.211x_1x_6 \\ &+ 1.607x_2x_6 + 0.705x_5x_6 + 0.560x_6^2 \\ &- 0.737x_1x_7 + 1.549x_2x_7 + 0.178x_5x_7 \\ &+ 1.817x_6x_7 + 2.144x_7^2 + 2.307x_1x_{eq} \\ &+ 0.475x_2x_{eq} - 2.849x_5x_{eq} - 0.440x_6x_{eq} \\ &+ 0.019x_1x_{eq} + 14.384x_{eq}^2 \end{aligned} \quad (2)$$

and

$$\begin{aligned}\hat{y}_{\sigma|\text{radial-bearing}} &= 6.192 + 0.408x_1 - 0.075x_2 - 1.156x_5 \\ &+ 0.011x_6 + 0.235x_7 + 12.910x_{eq} + 0.357x_1^2 \\ &+ 0.128x_1x_2 - 0.503x_2^2 - 0.012x_1x_5 \\ &+ 0.037x_2x_5 + 0.911x_5^2 + 0.142x_1x_6 \\ &+ 0.467x_2x_6 + 0.194x_5x_6 - 0.514x_6^2 \\ &- 0.253x_1x_7 + 0.369x_2x_7 - 0.062x_5x_7 \\ &+ 0.577x_6x_7 + 0.841x_7^2 + 0.682x_1x_{eq} \\ &+ 0.279x_2x_{eq} - 0.758x_5x_{eq} - 0.199x_6x_{eq} \\ &- 0.114x_1x_{eq} + 9.116x_{eq}^2 \end{aligned} \quad (3)$$

where $\hat{y}_{\mu|\text{radial-bearing}}$ is mean value of peak radial bearing deformation; $\hat{y}_{\sigma|\text{radial-bearing}}$ is one standard deviation for the peak radial bearing deformation; and x_1, x_2, x_5, x_6, x_7, and x_{eq} are random variables representing the number of spans, maximum span length, radius of curvature, girder spacing, cross-frame spacing, and earthquake intensity, respectively. To incorporate randomness with respect to earthquake excitations, final RSMs that incorporated both response functions can be expressed in Eq. (4).

$$\hat{y}_{\text{radial-bearing}} = \hat{y}_{\mu|\text{radial-bearing}} + N\left[0, \hat{y}_{\sigma|\text{radial-bearing}}\right] \quad (4)$$

Eq. (4) defines a random peak radial bearing deformation which is expressed as a mean value plus a zero-mean normal random variable having a standard deviation equal to that for the peak radial bearing deformation; values of peak radial bearing deformation can then be simulated using Eq. (4). Detailed information on RSMs for the other output variables can be found elsewhere [31].

3.5. RSMs efficiency and accuracy

RSM efficiency and accuracy was examined by comparing the fragility generation process and the seismic responses using nonlinear time history finite element analyses. Again, the RSMs were determined via least-square regression analysis of CCD table consisting of the input and output variables. RSMs were then used to yield a number of critical seismic response quantities that were used as a basis to generate the fragility curves. Although the fragility generation process using nonlinear time history analyses is an ideal approach to investigate a detailed seismic response and allow for creating fragility curves of populations of curved steel bridges, it becomes extremely time-consuming. This is because an excessive amount of computational cost has been associated with generation and implementation of nonlinear analyses for a large

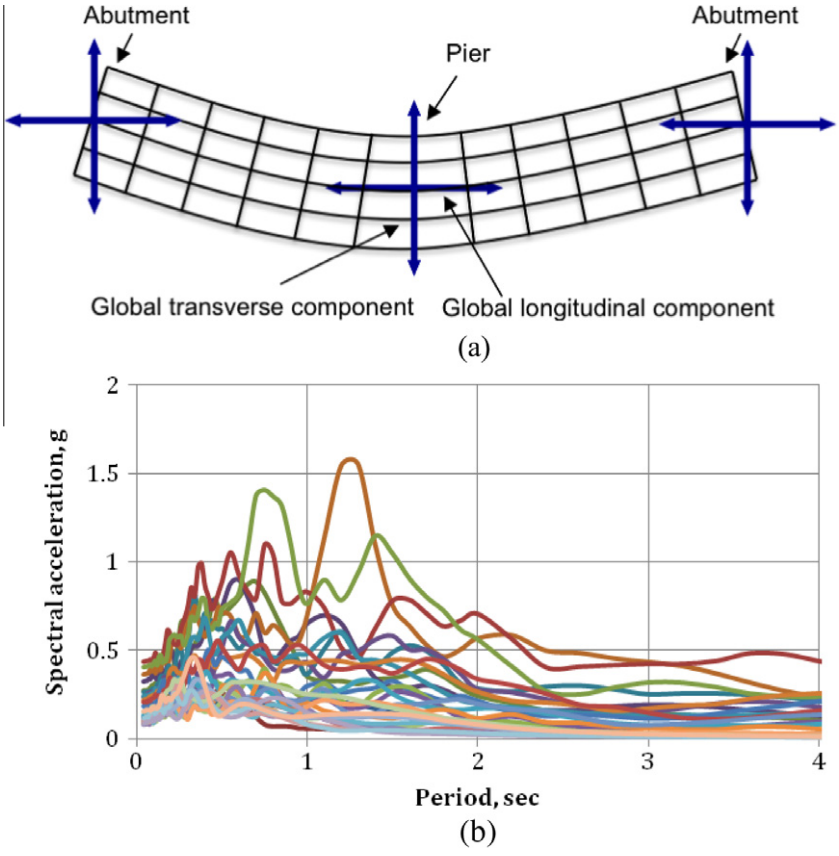

Fig. 6. (a) Seismic loading direction for nonlinear time history analysis; and (b) spectral accelerations of the synthetic ground motions.

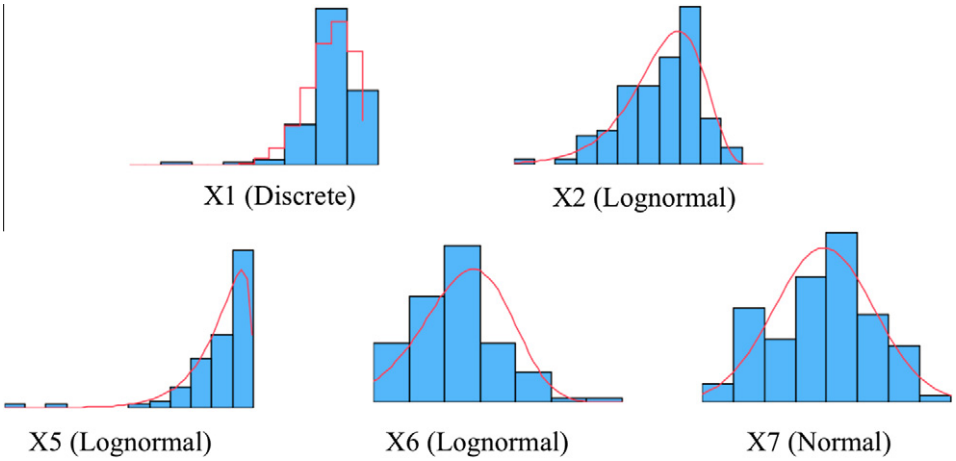

Fig. 7. Probability density functions for optimal curved bridge parameters.

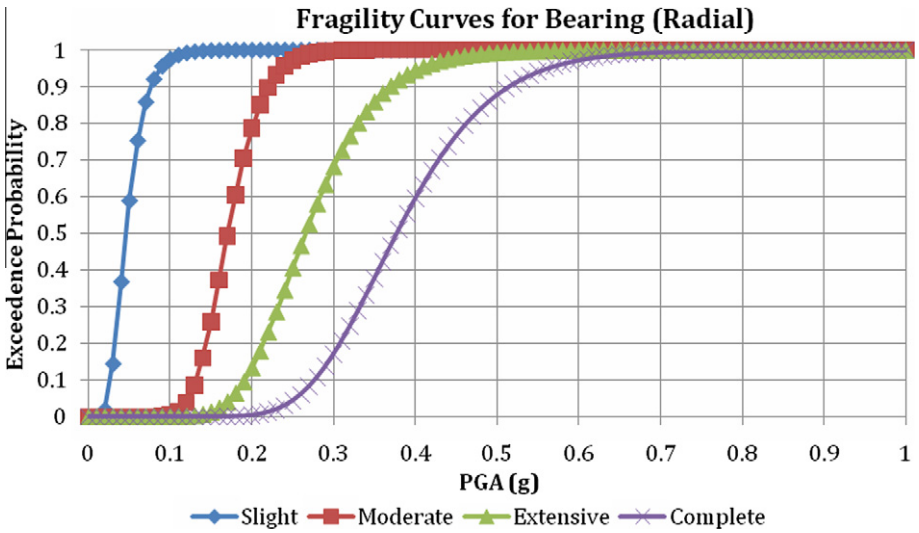

Fig. 8. Bearing radial deformation fragility curves.

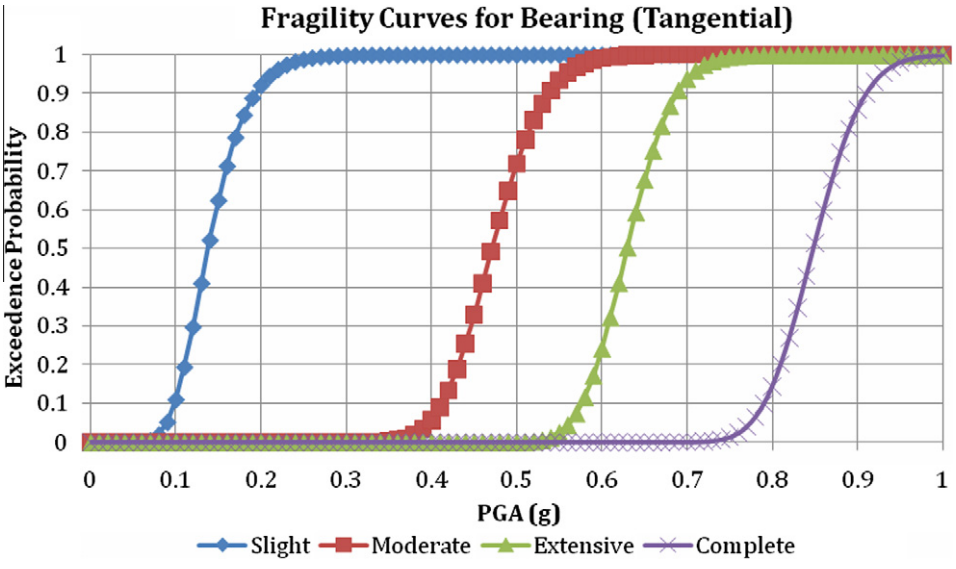

Fig. 9. Bearing tangential deformation fragility curves.

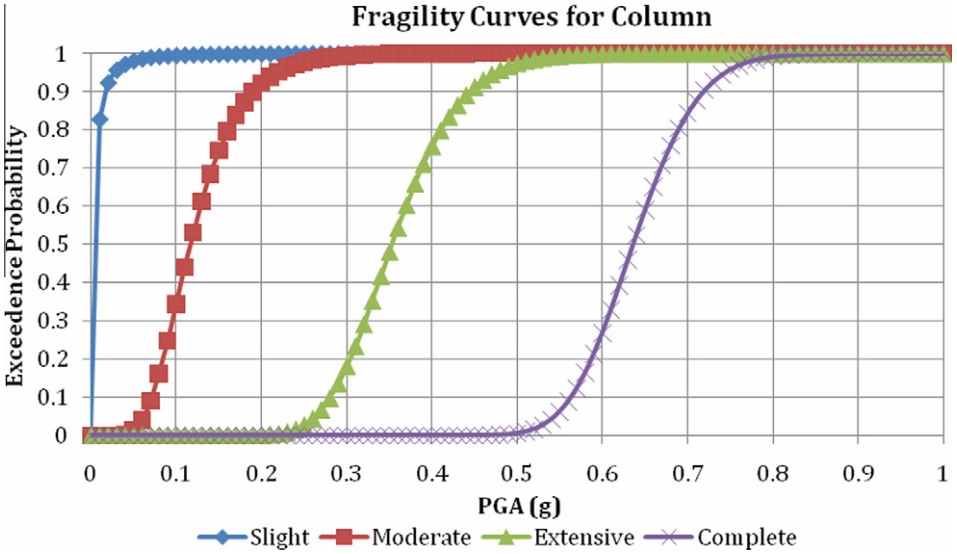

Fig. 10. Column curvature ductility fragility curves.

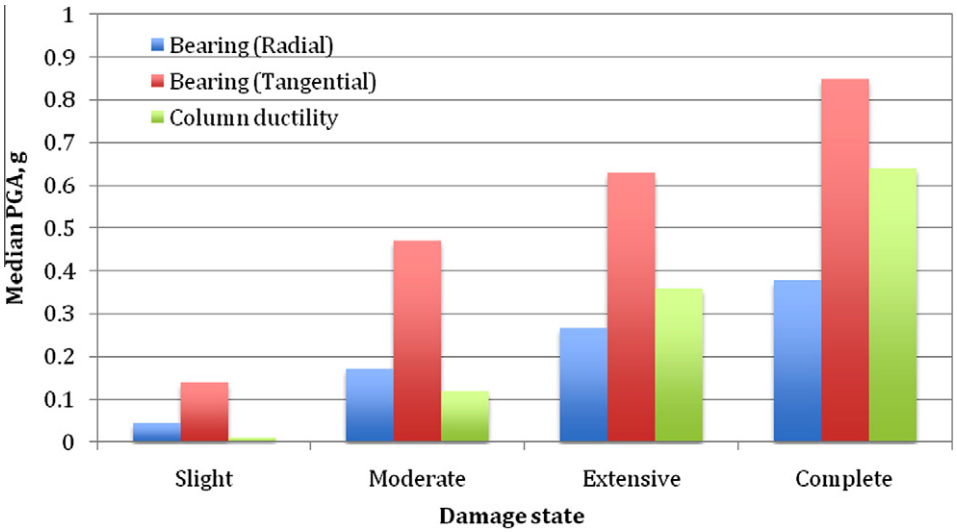

Fig. 11. Comparison of median PGA values of the fragility curves.

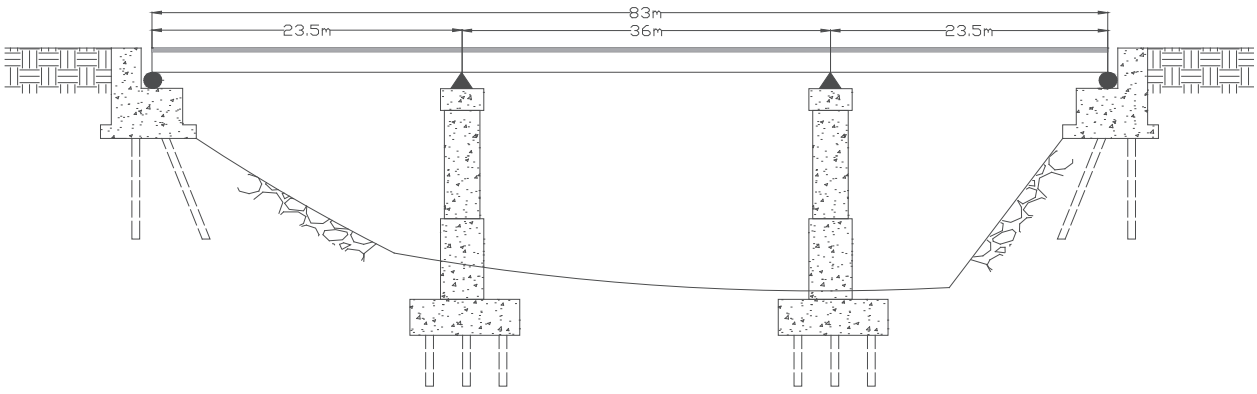

Fig. 12. Sample horizontally curved, steel, I-girder bridge.

population of curved bridges under a varying range of seismic hazards and with corresponding uncertainties included in the process.

For RSM accuracy validation, responses from the original curved steel bridge computational models were compared against corresponding RSM function results via examination of the root mean

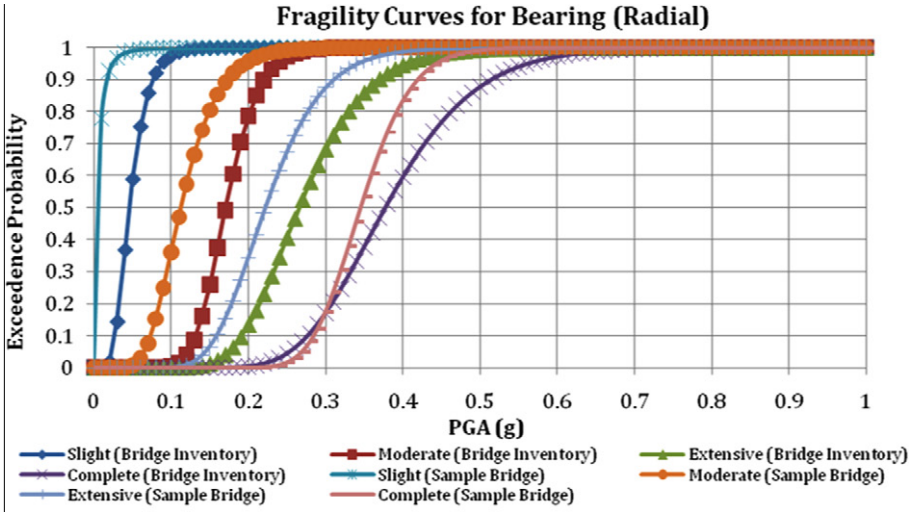

(a) Bearing radial deformation

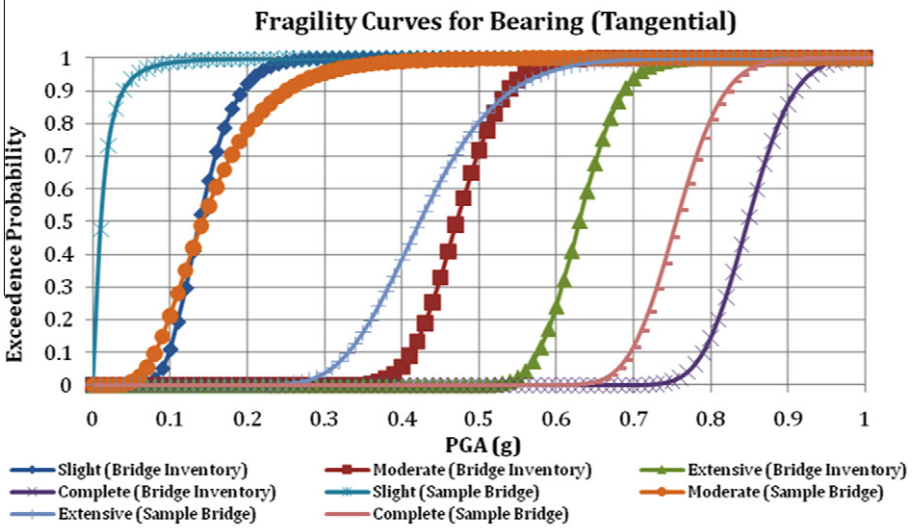

(b) Bearing tangential deformation

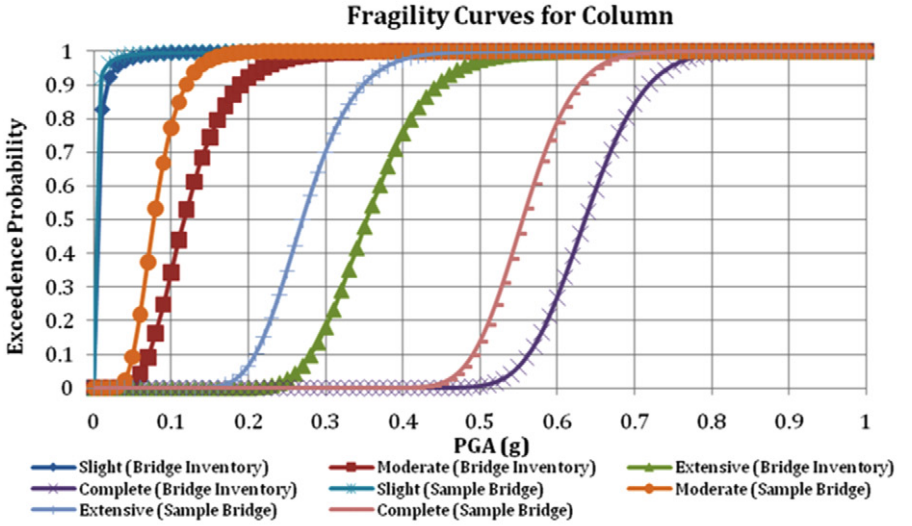

(c) Column ductility

Fig. 13. Comparison of fragility curves of bridge inventory and sample bridge.

square error. The error level varied between 5% and 10% and these discrepancies were deemed acceptable based on previous literature [32]. As a result of this examination, the application of RSMs allowed for fragility generation to be accomplished with good

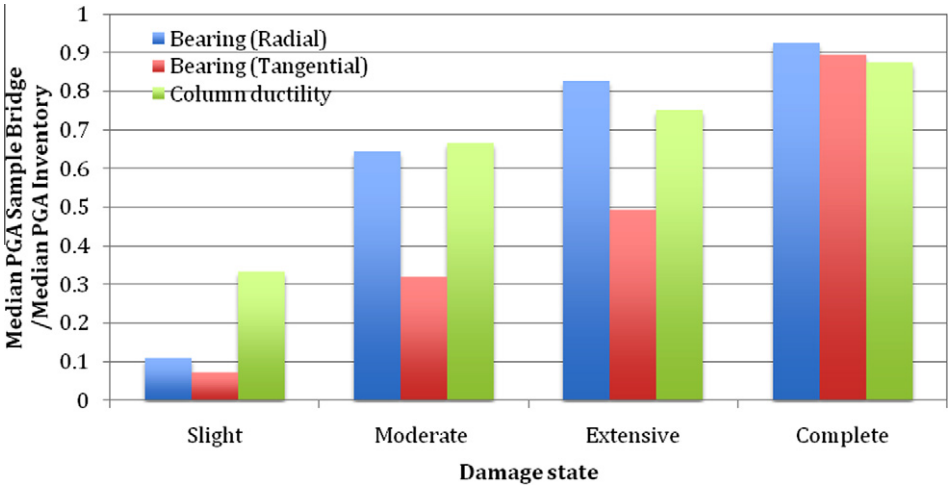

Fig. 14. Ratio of median PGA values of the fragility for sample bridge to bridge inventory.

accuracy at lower computational cost when compared to performing nonlinear time history analyses of a large number of curved bridge models.

3.6. RSM fragility curve development

The second application of the RSMs occurred when fragility curves were generated. They were used here to produce a large number of seismic responses that were used as a basis to develop the fragility curves. Those computed values were combined with Monte Carlo simulation to compute exceedance probabilities at different FEMA [25] performance states (i.e., slight, moderate, extensive, complete). Corresponding quantitative performance states were developed using an approach from previous research [5] that focused on the interpretation of critical bridge component behavior to develop bridge performance quantities corresponding to the qualitative FEMA performance states. Past research [3–6] has shown that the seismic damage to bridges commonly occurred at the bearings and in the abutments and supporting columns. The quantitative performance states were related to these critical response items. For horizontally curved bridge vulnerabilities, limiting performance quantities for the critical bridge components from previous work [5] were adjusted via vectoral modification based on the level of horizontal curvature. The Monte Carlo simulations were completed with the RSMs using 10,000 trial-runs, which were deemed an appropriate number of simulations to accurately derive fragility curves from previous research [13]. Output from the Monte Carlo simulations, which incorporated probability density functions (PDFs) from the five optimal input parameters, was compared to criteria from the adjusted performance state quantities to produce exceedance probabilities related to each seismic response output parameter. PDFs for each of the five optimal parameters are shown in Fig. 7. A discrete distribution was used for the number of spans ($X1$), a normal distribution was used for cross-frame spacing ($X7$) and lognormal distributions were used for the other parameters ($X2$, $X5$, and $X6$). These PDFs were representative of uncertainties of their inherent randomness for the set of 99 bridges that was initially studied.

Representative sets of seismic fragility curves are displayed in Figs. 8–10 for select bridge output parameters: the bearing radial and tangential deformations and column ductility curvature. The curves detail the likelihood of different performance levels, as defined by FEMA [25], being reached and exceeded as a function of PGA. As shown in Fig. 8 for bearing radial deformations, seismic fragility curves for each performance state reach an exceedance probability of 1 at different PGAs, with the slight damage curve reaching 1 for PGAs between 0.1 g and 1 g, the moderate damage curve reaching 1 for PGAs between 0.25 g and 1 g, the extensive damage curve reaching 1 for PGAs between 0.46 g and 1 g, and the complete damage curve reaching 1 for PGAs between 0.7 g and 1 g. In Fig. 9 for bearing tangential deformations, the fragility curve for the slight damage level has an exceedance probability of 1 for PGAs between 0.24 g and 1 g, the moderate curve for PGAs between 0.6 g and 1 g, the extensive curve for PGAs between 0.74 g and 1 g, and the complete curve for PGAs between 0.96 g and 1 g. These results indicate that slight to severe bearing damage could possibly occur for curved bridges in the studied regions (e.g., Pennsylvania, Maryland, and New York) during low to moderate earthquakes with PGAs between 0.1 g and 0.3 g in. As shown in Fig. 10 for column curvature ductility, the slight damage level fragility curve has an exceedance probability of 1 over all PGAs. This indicates that slight column damage could possibly occur during minor earthquakes for curved bridges in the studied regions (e.g., Pennsylvania, Maryland, and New York).

Via comparisons between these curves and similar curves generated for abutment radial and tangential deformations components that appear more sensitive to damage at certain PGAs can be identified. Details on the other fragility curves can be found elsewhere [31]. Based on these comparisons, column curvature ductility appeared to be the component that would be most susceptible to slight to moderate damages for the studied curved steel bridge inventory, while bearing radial deformations appeared to be the most susceptible to extensive to complete damage [31]. To better illustrate this trend, the median PGA values of the fragility curves for different damage states is plotted in Fig. 11. It indicated that a smaller median PGA value of component resulted in a higher vulnerability in the fragility curves.

3.7. RSM fragility curve application

To better understand the use of the proposed fragility development methodology, it was applied to generate curves for a single horizontally curved bridge not used in this study and the fragilities obtained for this bridge were compared to those generated from the initial inventory of 99 bridges. As shown in Fig. 12, the selected bridge structure is a three-span continuous bridge with a radius of curvature of 380 m, a maximum span length of 36 m, a cross-frame spacing of 4.5 m, and a girder spacing of 2.5 m.

To observe vulnerability of the sample bridge, comparisons between inventory and sample fragility curves were completed. Fig. 13a–c show representative comparisons of fragility curves for the slight to complete damage states for the entire inventory

and sample bridge for the bearing tangential and radial deformation as well as column ductility curvature. It appears that the overall vulnerability of the sample bridge is higher than that for the bridge inventory when bearing and column are considered. This implies that the seismic response of the sample bridge at a given PGA is larger than that for the inventory. A quantitative comparison between the two fragilities occurred by looking at a ratio of median PGA values for the sample bridge fragility curves to those that for the inventory. Fig. 14 shows the ratio plot at different damage states. In this figure, a smaller ratio is indicative of a sample bridge component resulting in higher vulnerability relative to the inventory. For example, the ratio for the bearing tangential deformation fragility was approximately 0.07 at the slight damage state while the sample bridge vulnerability increased by 92% relative to the inventory on the basis of the median value shift. This type of result could assist with prioritizing seismic retrofits for a specific bridge.

4. Conclusions

The study described herein proposed the use of a RSM methodology in conjunction with Monte Carlo simulation for the generation of horizontally curved steel bridge seismic fragility curves that examined certain critical output components (i.e. at the bearings, abutments and pier columns). The curves were generated using statistical information from an inventory of horizontally curved steel bridges located in Pennsylvania, Maryland, and New York. Optimal parameters used to develop the RSMs were determined using statistical screening and the fragility curves were created via Monte Carlo simulation that incorporated the developed RSMs. To better understand the use of this methodology, it was applied to a single curved bridge not used in inventory to generate fragility curves and those fragilities were compared to fragilities generated from the inventory of 99 bridges. In addition to illustrating the use and possible computational benefits resulting from this technique, the resulting fragilities indicated that:

(1) Column curvature ductility appears to be the most susceptible component at the slight to moderate damage states for the bridge inventory that was studied.
(2) Bearing radial deformations are the most vulnerable components at the extensive to complete damage states for the inventory that was studied.
(3) Slight to severe column and bearing damage could occur during earthquakes with PGAs between 0.1 g and 0.3 g for the inventory that was studied.

Possible advantage to implementing this methodology is its computational efficiency via the elimination of a large number of nonlinear time history finite element analyses. Resulting fragility curves can assist with identifying vulnerable bridge components over a large seismic intensity range. As a result, they could aid bridge management decision-making by helping to prioritize seismic strengthening repairs.

Acknowledgements

Funding for this work is provided by the Korea Electric Power Infrastructure Center. The Pennsylvania, Maryland, and New York Departments of Transportation are gratefully acknowledged for providing access to existing horizontally curved steel I-girder bridge plan sets.

References

[1] Murachi Y, Orikowski MJ, Dong X, Shinozuka Y. Fragility analysis of transportation networks. Smart Structures and Material. San Diego (CA); 2003.
[2] Shinozuka M, Feng Maria Q, Kim HK, Kim SH. Nonlinear static procedure for fragility curve development. Journal of Engineering Mechanics 2000;126(12):1287–96.
[3] Choi E, DesRoches R, Nielson B. Seismic fragility of typical bridges in moderate seismic zones. Engineering Structure 2004;26(2):187–99.
[4] Padgett JE, DesRoches R. Methodology for the development of analytical fragility curves for retrofitted bridges. Earthquake Engineering and Structural Dynamics 2008;37(8):1157–74.
[5] Nielson BG, DesRoches R. Analytical fragility curves for typical highway bridge classes in the Central and Southeastern United States. Earthquake Spectra 2007;23(3):615–33.
[6] Nielson BG, DesRoches R. Seismic fragility methodology for highway bridges using a component level approach. Earthquake Engineering and Structural Dynamics 2007;36:823–39.
[7] ATC. Earthquake damage evaluation data for California. Report No. ATC-13, Applied Technology Council, 1985.
[8] Basoz N, Kiremidjian, Anne S. Evaluation of bridge damage data from the Loma Prieta and Northridge (CA) earthquakes. Report No. MCEER-98-0004, MCEER; 1997.
[9] Shinozuka M, Feng MQ, Lee J, Naganuma T. Statistical analysis of fragility curves. Journal of Engineering Mechanics 2000;126(12):1224–31.
[10] Wu CFJ, Hamada M. Experiments-planning, analysis and parameter design optimization. John Wiley & Sons; 2000.
[11] de Felice G, Giannini R. An efficient approach for seismic fragility assessment with application to old reinforced concrete bridges. Journal of Earthquake Engineering 2010;14(2):231–51.
[12] Rossetto T, Elnashai AS. A new analytical procedure for the derivation of displacement-based vulnerability curves for populations of RC structures. In: the 13th World Conference on Earthquake Engineering, Paper No. 1006. Vancouver (BC); 2004.
[13] Park J, Towashiraporn P, Craig J, Goodno B. Seismic fragility analysis of low-rise unreinforced masonry structures. Engineering Structures 2009;31(1):125–37.
[14] Dueñas-Osorio L, Craig JI, Goodno BJ. Rapid regional response simulation of 3-D prototype structures for fragility characterization. In: the 13th World Conference on Earthquake Engineering, Paper No. 1499. Vancouver (BC); 2004.
[15] Franchin P, Lupoi A, Pinto PE. Seismic fragility of reinforced concrete structures using a response surface approach. Journal of Earthquake Engineering 2003;7(NSI):45–77.
[16] FHWA. National bridge inventory data website, http://www.fhwa.dot.gov/BRID GE/britab.cfm; 2008 [accessed 20.08.08].
[17] Davidson JS, Abdalla RS, Madhavan M. Design and construction of modern curved bridges. Report No. FHWA/CA/OR. University Transportation Center for Alabama, The University of Alabama; 2002.
[18] Brockenbrough RL. Distribution factors for curved I-girder bridges. Journal of Structural Engineering 1986;112(10):2200–15.
[19] Chang CJ, White DW. An assessment of modeling strategies for composite curved steel I-girder bridges. Engineering Structures 2008;30(11):2991–3002.
[20] Kim WS, Laman JA, Linzell DG. Live load radial moment distribution for horizontally curved bridges. Journal of Bridge Engineering 2007;12(6):727–36.
[21] Abdel-Salam MN. Seismic response of curved steel box girder bridges. Journal of Structural Engineering 1988;114(12):2790–800.
[22] Cundy AL, Hemez FM, Inman DJ, Park G. Use of response surface metamodels for damage identification of a simple nonlinear system. Key Engineering Materials 2003;245–246:167–74.
[23] Rix GJ, Fernandez-Leon JA. Synthetic ground motions for Memphis (TN). http://www.ce.gatech.edu/research/mae_ground_motion; 2004 [accessed 05.06.08].
[24] Mazzoni S, McKenna F, Scott MH, Fenves GL, et al. Open system for earthquake engineering simulation (OpenSees). Pacific Earthquake Engineering Research Center, Version 1.7.3; 2008.
[25] FEMA. HAZUS-MH MR1: Technical manual. Federal Emergency Management Agency. Vol. Earthquake Mode. Washington, DC; 2003.
[26] Hwang H, Jernigan JB, Lin YW. Evaluation of seismic damage to Memphis bridges and highway systems. Journal of Bridge Engineering 2000;5(4):322–30.
[27] Mander JB, Kim DK, Chen SS, Premus GJ. Response of steel bridge bearings to the reversed cyclic loading. Report No. NCEER 96-0014. NCEER; 1996.
[28] Azizinamini A, Pavel R, Lotfi HR. Effect of cross bracing on seismic performance of steel I-girder bridges. In: Proceedings of Structures Congress XV: Building to Last, SEI-ASCE; 1996.
[29] Montgomery DC. Design and analysis of experiments. John Wiley & Sons, Inc.; 1997.
[30] SAS Institute Inc. JMP statistics and graphics Guide – Version 5.1.2. Cary, NC; 2008.
[31] Seo JW. Seismic vulnerability assessment of a family of horizontally curved steel bridges using response surface metamodels. Ph.D. Dissertation. Pennsylvania State University; 2009.
[32] Engelund WC, Stanley DO, Lepsch RA, McMillin MM, Unal R. Aerodynamic configuration design using response surface methodology analysis. In: Proceedings of the AIAA Aircraft Design, Systems, and Operations Meeting, Monterey, CA; 1993.